Segregation of Photosystems in Thylakoid Membranes as a Critical Phenomenon

Igor Rojdestvenski,* Alexander G. Ivanov,†‡ M. G. Cottam,§ Andrei Borodich,* Norman P. A. Huner,‡ and Gunnar Öquist*

*Department of Plant Physiology, Umeå University, Umeå S-90 187, Sweden; †Institute of Biophysics, Bulgarian Academy of Sciences, Sofia 1113, Bulgaria; and ‡Department of Plant Sciences and §Department of Physics and Astronomy, University of Western Ontario, London N6A 5B7, Canada

ABSTRACT The distribution of the two photosystems, PSI and PSII, in grana and stroma lamellae of the chloroplast membranes is not uniform. PSII are mainly concentrated in grana and PSI in stroma thylakoids. The dynamics and factors controlling the spatial segregation of PSI and PSII are generally not well understood, and here we address the segregation of photosystems in thylakoid membranes by means of a molecular dynamics method. The lateral segregation of photosystems was studied assuming a model comprising a two-dimensional (in-plane), two-component, many-body system with periodic boundary conditions and competing interactions between the photosystems in the thylakoid membrane. PSI and PSII are represented by particles with different values of negative charge. The pair interactions between particles include a screened Coulomb repulsive part and an exponentially decaying attractive part. The modeling results suggest a complicated phase behavior of the system, including quasi-crystalline phase of randomly distributed complexes of PSII and PSI at low ionic screening, well defined clustered state of segregated complexes at high screening, and in addition, an intermediate agglomerate phase where the photosystems tend to aggregate together without segregation. The calculations demonstrated that the ordering of photosystems within the membrane was the result of interplay between electrostatic and lipid-mediated interactions. At some values of the model parameters the segregation can be represented visually as well as by analyzing the correlation functions of the configuration.

INTRODUCTION

The chloroplasts of most photosynthetic organisms contain continuous thylakoid membrane system differentiated into granal stacks consisting of appressed thylakoid discs that are interconnected by non-appressed stromal thylakoids (Goodchild et al.; 1972; Anderson, 1999). In the thylakoid membranes two types of photosystems are embedded. Photosystems are pigment-protein complexes, which transform the energy of the light quanta into charge separation, vital for plant metabolism. Both types of photosystems differ in size (Staehelin and Arntzen, 1983), pigment and protein composition (Glazer and Melis, 1987), and charge (Barber, 1982; Chow et al., 1991).

A characteristic feature of the photosynthetic thylakoid membranes of higher plants and some green algae is the spatial separation of photosystem I (PSI) and photosystem II (PSII) within the grana and stroma lamellae. Thylakoids of grana stacks are mostly abundant in PSII complexes, while PSI complexes are predominant in stroma lamellae (Andersson and Anderson, 1980; Anderson and Andersson, 1982; Chow et al., 1991; Anderson, 1999). Such spatial separation of two types of photosystems is called lateral segregation.

Although the differentiation of the thylakoids into grana and stroma membrane regions is viewed as a morphological reflection of the non-random distribution of the PSII and PSI chlorophyll-protein complexes between appressed (grana) and non-appressed (stroma) membrane domains, the possible physiological significance of this phenomenon (Anderson, 1999) and the mechanisms controlling the lateral heterogeneity (Chow et al., 1991; Chow, 1999) are still a matter of discussion. The degree of thylakoid membrane stacking and the simultaneous lateral segregation of PSII and PSI complexes depend strongly on the environmental conditions in vivo (Anderson, 1999). It has been suggested that the lateral heterogeneity and the formation of grana serve the purpose of physical separation of slow (PSII) and fast (PSI) photosystems allowing the regulation of the distribution of excitation energy over the two photosystems (Anderson, 1982; Trissl and Wilhelm, 1993). More recently, grana stacking was hypothesized to play an important role in protecting PSII under condition of sustained high light irradiance (Anderson and Aro, 1994).

The phenomenon of grana formation proper is not within the scope of our paper. However, the topology of the grana disks is likely to be of importance when the grana formation proper is studied. For the formation of the disks themselves a spontaneous breaking of translational symmetry in the lateral distribution of the protein complexes in the membrane is needed. In Barber (1982) and Stys (1995) it is also discussed that the heterogeneity of protein distribution serves as the necessary condition for grana formation. Some experiments suggest (Wollman and Diner, 1980; Rubin et al., 1981) that segregation of proteins in thylakoid membrane and lamella stacking are consequent events in grana

Submitted June 22, 2001, and accepted for publication January 17, 2002.

Address reprint requests to Dr. I. Rojdestvenski, Department of Plant Physiology, Umeå University, S-90187, Sweden. Tel.: 46-70-7195291; Fax: 46-90-7866676; E-mail: igor.rojdestvenski@plantphys.umu.se.

0006-3495/02/04/1719/12 $2.00

formation. Therefore, different scenarios of clustering and segregation may affect the grana formation.

It has been demonstrated in early studies that at low salt zwitterionic buffer the spinach chloroplasts had not exhibited the characteristic stacked thylakoids (Izawa and Good, 1966) and the chlorophyll protein complexes of PSII and PSI are homogeneously distributed within the thylakoid membranes (Ojakian and Satir, 1974). Under these conditions the excitation energy transfer between PSII and PSI (spillover) is facilitated and a low level of chlorophyll *a* fluorescence is observed (Murata, 1969; Butler, 1978). Addition of cations leads to the electrostatic screening of negative surface charges, thus causing restacking of thylakoids, followed by lateral segregation of PSII and PSI complexes, resulting in a decrease of PSII to PSI excitation transfer and an enhancement of PSII fluorescence (Barber and Chow, 1979; Anderson, 1981). Studies that combined fluorescence measurements and electron microscopy showed that the degree of spillover strongly depends on the extent of thylakoid stacking and segregation of photosystems in the membrane and the distances between them (Barber et al., 1980; Braintais et al., 1984; Ivanov and Apostolova, 1997). The results of fluorescence kinetics experiments also suggest that the segregation and restacking are independent phenomena, occurring via two different ion-dependent mechanisms (Wollman and Diner, 1980; Braintais et al., 1984; Stys, 1995).

It has been previously hypothesized on a possible dominant role of the electrostatic interactions in segregation and stacking phenomena, as well as of kinetic properties of PSI and PSII diffusion in the membrane (Barber, 1982; Ivanov et al., 1987; Chow et al., 1991). More recently, Stys (1995) introduced the concept of protein/lipid hydrophobic matching (hydrophobic mismatch) (Mouritsen and Bloom, 1993) for better understanding of the forces responsible for dynamic cation-induced stacking and segregation phenomena. In fact, a number of experimental evidences have demonstrated that alterations in membrane dynamic properties and/or lipid composition of the thylakoid membranes correlated with changes in the degree of membrane stacking (Ivanov, 1991) and energy distribution between the two photosystems (Yamamoto et al., 1981; Haworth, 1983; Ivanov and Apostolova, 1997; Dobrikova et al., 1997).

There are two main approaches in explaining the cation-induced PSI-PSII segregation. One is represented by the surface charge (SC) theory (Barber 1982), which attributes segregation and stacking to cooperative phenomena in ensembles of electrostatically interacting lipids and pigment-protein complexes. Another approach is molecular recognition (MR) theory (Allen, 1992). MR theory attributes the cation-dependent segregation and stacking to changes in protein structures and, hence, their binding specificities.

The pigment-protein complexes within the membrane interact via Coulomb interactions (screened in the presence of cations), van der Waals (VDW) forces, dipole-dipole interactions, and lipid-induced protein-protein attraction (Kleinschmidt and Marsh, 1997; Ben-Tal et al., 1997; Sintes and Baumgartner, 1997). In a semi-microscopic treatment we view the lipid membrane as a continuous medium, which may be taken, depending on the chosen theoretical approach, either as a fluid or elastic medium (see, e.g., Israelachvili, 1992; Gennis, 1989). Within the framework of these approaches the Coulomb electrostatic force and VDW-type and elastic electrodynamic forces are most important. In our simulations we have taken the repulsive part of the effective long-range pair potential as screened Coulomb and the attractive long-range one as lipid-mediated interactions between proteins. Lipid-mediated interactions partially overlap with long-range VDW-type and elastic forces because of the fluctuation contributions (Marcelja, 1976; Mouritsen and Bloom, 1993; Heimburg and Biltonen, 1996). Also these interactions include some effects due to the entropic contributions of oscillating hydrophobic and solvation forces, such as hydrophobic matching of proteins and lipids and formation of depleted zones around proteins (Chow, 1999; Sintes and Baumgartner, 1997). In particular, Sintes and Baumgartner (1997) found two types of lipid-mediated attraction between proteins embedded in a bilayer membrane: a short-range depletion-induced attraction and a long-range fluctuation-induced attraction. The presence of competing attractive and repulsive interactions can qualitatively explain the effects of divalent cations, trypsin, and high-temperature treatments on the protein-protein interactions by changing the interactions between photosystems.

MODEL FOR THE PSI/PSII INTERACTIONS WITHIN THE MEMBRANE

When discussing the possible model interactions of the protein complexes within the membrane it is vital to define accurately the chosen level of description. The highest level of description is normally the thermodynamic, macroscopic level. Hence the general thermodynamic properties of the system are determined, but it is impossible to obtain any detailed information about the microscopic kinetics of the system and its microscopic equilibrium state. This is the level of description at which the concept of entropic forces is widely utilized. On the other hand, a purely microscopic approach (see, e.g., Sintes and Baumgartner, 1997), in which the ensemble consists not only of the protein particles, but the lipid particles as well, is quite heavy computationally for any reasonable size of the investigated system. In our work we chose an intermediate approach. Namely, the dynamical behavior of the protein particles is treated microscopically. Then we postulate the effective interactions between the particles in the system as a result of macroscopic thermodynamic approach for the screened Coulomb interaction (with the thermodynamic treatment of the ensemble of cations around the proteins) as well as for

the indirect interactions via the lipid media (which is also treated thermodynamically).

Thylakoid grana lamellae represent flattened sacs with diameter of ~0.5–0.8 μm (Barber, 1982). The membrane thickness does not exceed 100 Å, and the maximal size of a protein complex embedded in it is ~100–150 Å (Wollman et al., 1999). Thus it is a reasonable approximation to consider the lipid bilayer as a flat, two-dimensional surface.

As in the work by Rojdestvenski et al. (2000) we neglect any deviations from pairwise spherically symmetric interactions that may be present in real systems due to the asymmetry of pigment-protein complexes or arise as extra non-pairwise entropic terms in the thermodynamics based treatments of the lipid-induced protein-protein interactions. Further, we assume that the photosystems carry negative charges of -1.6×10^{-18} C (PSI) and -1.2×10^{-18} C (PSII) and can move within a two-dimensional plaquette 0.6×0.6 μm^2 (which is approximately four times the granal vesicle size) with periodic boundary conditions representing the thylakoid membrane. Data for the thylakoid membrane surface charge density (Barber, 1982) confirm the correct order of magnitude of these values. We neglect the effects of membrane plane curvature on the diffusion properties of particles and take the lipid membrane to be electrically neutral (Quinn and Williams, 1983). The total number of particles in the system was taken to be 800 (corresponding to a typical density of 2000–3000 particles/μm^2) (Haehnel, 1984; Drepper et al. 1993) with the PSII to PSI ratio being 7:3, which is consistent with the commonly accepted value of ~2:1 for higher plant chloroplasts (Staehelin, 1986; Chow et al., 1991). We postulate that the total interaction potential between particles is the sum of a Debye-type repulsion U_C and a lipid-induced attraction U_L (Sintes and Baumgartner, 1997):

$$U_c(r) = \frac{q_1 q_2}{4\pi\varepsilon_0\varepsilon}\frac{e^{-r/\xi}}{r}; \quad U_L(r) = -\lambda k_B T e^{-r/\zeta};$$

$$\xi^{-1} = \sqrt{\frac{2Z^2\bar{n}e^2}{k_B T\varepsilon_0\varepsilon}}, \qquad (1)$$

where $q_{1,2}$ are effective charges of the PSI and PSII particles, whereas r and ξ are the interparticle distance and Debye length, respectively. ε represents the dimensionless dielectric permeability of the medium around the membrane, and $\bar{n}$ and Ze denote the ionic strength and the charge of an ion, respectively. The dielectric permeability of the medium is, in our case, hard to estimate. On one hand, the dielectric permeability of water is typically 50–100 depending on the environment. On the other hand, in the vicinity of a membrane or a pigment-protein complex it can be much lower (10–20) (see, e.g., White and Wimley, 1999). In our calculations we chose $\varepsilon = 50$. The quantity $k_B T$ is the temperature in energy units, λ represents the dimensionless strength of the attraction, and ζ is the characteristic length of the lipid-induced attraction. Parameter λ incorporates the dependence of this interaction on temperature, geometry, photosystems' structure, and membrane lipid composition. The fluctuation nature of this attraction makes it reasonable to measure its strength in the units of $k_B T$, hence the coefficient in Eq. 1. Because it is not possible to estimate λ ab initio, we choose it as a free parameter. Another free parameter of the calculation was the Debye length, ξ, which is used instead of the explicit value for the ionic strength (because of not knowing the exact value of ε).

Finally, we account for the diffusion by adding a random displacement component with an amplitude according to a diffusion coefficient, which we took as $D = 6 \times 10^{-12}$ cm^2 s^{-1} at 20°C (Rubin et al. 1981). The viscosity of the system is considered to be high enough to exclude acceleration terms from the equations of motion.

We should mention here that in this paper we resorted to the simplest types of interactions. The aim of this paper is to show that clustering and segregation phenomena can be explained as a phase transition in the ensemble of photosystems within the membrane with quite simple interactions (see, e.g., Stanley, 1988). A detailed study of the same system with several other types of interactions will be published elsewhere (A. Borodich, I. Rojdestvenski, A. Ivanov, N. Huner and G. Öquist, manuscript in preparation).

Modeling routine

We employ a variable time step molecular dynamics calculation scheme that is slightly different from the one described by Rojdestvenski et al. (2000). The modifications are incorporated here to compensate for the dynamical slowdown when the system is close to clustering.

For each calculation the particles are initially randomly distributed within the plaquette, which has the linear size of $L = 0.6$ μm. We also set up a maximal possible displacement, Δr_{max}, of a particle during a single step, as well as the seed time step, Δt_s. The choice of Δr_{max} and Δt_s is a compromise between the speed of calculations and the required accuracy. In our case we chose Δr_{max} to be $0.0125L$ (that is about the actual size of a single photosystem) and $\Delta t_s = 1$ ms. Each step of the calculation comprises the following operations. 1) We calculate the resulting force of interaction of each particle, i, with all the others in the ensemble, including their eight closest images in the neighboring plaquettes. 2) After the x- and y-components of the resultant force $F^i_{x,y}$ are calculated, they are converted into the components of seed displacement due to the interaction:

$$\Delta r^{is}_{x,y} = F^i_{x,y} D \Delta t_s / k_B T; \quad \Delta r^{is} = \sqrt{(\Delta r^{is}_x)^2 + (\Delta r^{is}_y)^2}$$

3) Then the actual time interval and the actual displacements due to interaction for each particle are calculated as:

$$\Delta t = \Delta t_s \frac{\max_i(\Delta r^{is})}{\Delta r_{max}}; \quad \Delta r^{i,int}_{x,y} = \Delta r^{is}_{x,y}\frac{\max_i(\Delta r^{is})}{\Delta r_{max}},$$

where the maximum is calculated over the displacements of all the particles. 4) Finally we calculate the displacement due to diffusion as:

$$\Delta r^{iD}_{x,y} = \sqrt{2D\Delta t v^{i}_{x,y}},$$

with $v^{i}_{x,y}$ being randomly chosen from the discrete set of numbers $\{-1, 0, 1\}$. 5) Then each particle is moved by an amount

$$\Delta r^{i,total}_{x,y} = \Delta r^{i,int}_{x,y} + \Delta r^{iD}_{x,y}$$

with the periodic boundary conditions taken into account. 6) After all the particles are moved the running value of the modeling time is increased by Δt.

In a single calculation the above routine was applied as a sequence of runs with fixed values of the parameters. We first defined the values of λ and ζ, which would be constant throughout the calculation. Then we accomplished 30–100 series with fixed values of the Debye radius ξ, beginning from a certain initial value ξ_o, dumping configuration and correlation function data approximately every 10 μs of the modeling time. Then the calculation was repeated several times with the ξ value subsequently decreased and initial configuration taken from the final configuration of the previous run. The correlation functions were averaged over each 10-μs time portion.

In the course of the calculations it turned out that the diffusion displacements were, in most cases, much smaller than the displacements due to the interaction. This provided for the stability of the obtained configurations.

For visualizing the resulting configurations we used the virtual reality markup language (VRML). The configuration pictures in Figs. 1–6 are the screenshots of the VRML configuration files viewed using appropriate VRML Browser.

RESULTS AND DISCUSSION

We find that, depending on the values of the model parameters, there are several scenarios for the systems' kinetics. These scenarios may be observed either by analyzing the correlation functions of the system or directly by looking at the resulting configurations. Specifically, our calculations suggest that the clustering and the segregation are separate processes that may have, at different parameter values, quite different characteristic times. Several resulting configurations are possible as a result of the interplay between these processes, as described below.

Simultaneous clustering and segregation

This situation occurs when the characteristic times of clustering and segregation are comparable, so both processes take place simultaneously. In Fig. 1 we present the results of calculations for a high value λ of the attractive interaction parameter. Clustering and segregation, at least within the time resolution of the numerical experiment, cannot be separated in time. This results in the system proceeding from an initial non-segregated crystalline-like phase (Fig. 1 *C*) into a phase where clusters are formed. Within the clusters the PSIIs form the core, and the PSIs form a peripheral belt (Fig. 1 *D*). PSII-PSI correlation functions of the initial and final states are presented in Fig. 1 *A*. A gradual crossover from the quasi-periodic behavior characteristic for crystal-like structures to an almost single maximum pertinent to segregated systems is clearly seen. We also looked in more detail at the dynamics of the first maximum of the correlation function (see the inset in Fig. 1 *A* together with Fig. 1 *B*). In the course of time evolution the first maximum gradually shifts toward lower values of distance, thus reflecting a more dense packing of particles in the clustered phase. The process of segregation, i.e., redistribution of particles, is reflected by the decrease of the height of the first maximum. We also note here that the situation presented in Fig. 1 may be termed as weak clustering because the clustering and segregation occurs at high values of the Debye radius, ξ, due to the substantial attraction radius, ζ, and attraction strength, λ.

A similar situation is presented in Fig. 2, where, at the same attraction strength, the clustering and segregation are also almost simultaneous. However, there can be a clear, although short, intermediate phase as seen in the configuration (Fig. 2 *C*) and in the correlation function plot (Fig. 2 *A*, triangles). This intermediate phase shows that clustering happens slightly faster than segregation, thus demonstrating that our division into different scenarios is not rigid. The same phenomenon can be seen in the inset in Fig. 2 *A*, which shows slight oscillations of the first maximum's height and location at around 50 μs. We term the clustering in Fig. 2 as strong, because the packing in the clustered state is much denser than in Fig. 1. We may speculate that the packing density is mostly dependent on the characteristic attraction radius, which is smaller in the case of Fig. 2 than in Fig. 1.

Clustering with delayed segregation

This scenario is characterized by noticeably different characteristic times of clustering and segregation, with clustering being much faster. In this case the intermediate phase is clearly identifiable. The example of such a situation is presented in Fig. 3. First, on the level of configuration (Fig. 3 *C*), the intermediate phase represents clustering without segregation. Then, in the course of further time evolution, a redistribution of particles takes place, resulting in the configuration shown in Fig. 3 *D*. The same effects are visible on the level of PSI-PSII correlation functions (Fig. 3, *A* and *B*). In Fig. 3 *A*, all three possible types of correlation functions can be seen. As before, the correlation function of the initial state is quasi-periodic, which is characteristic of the non-

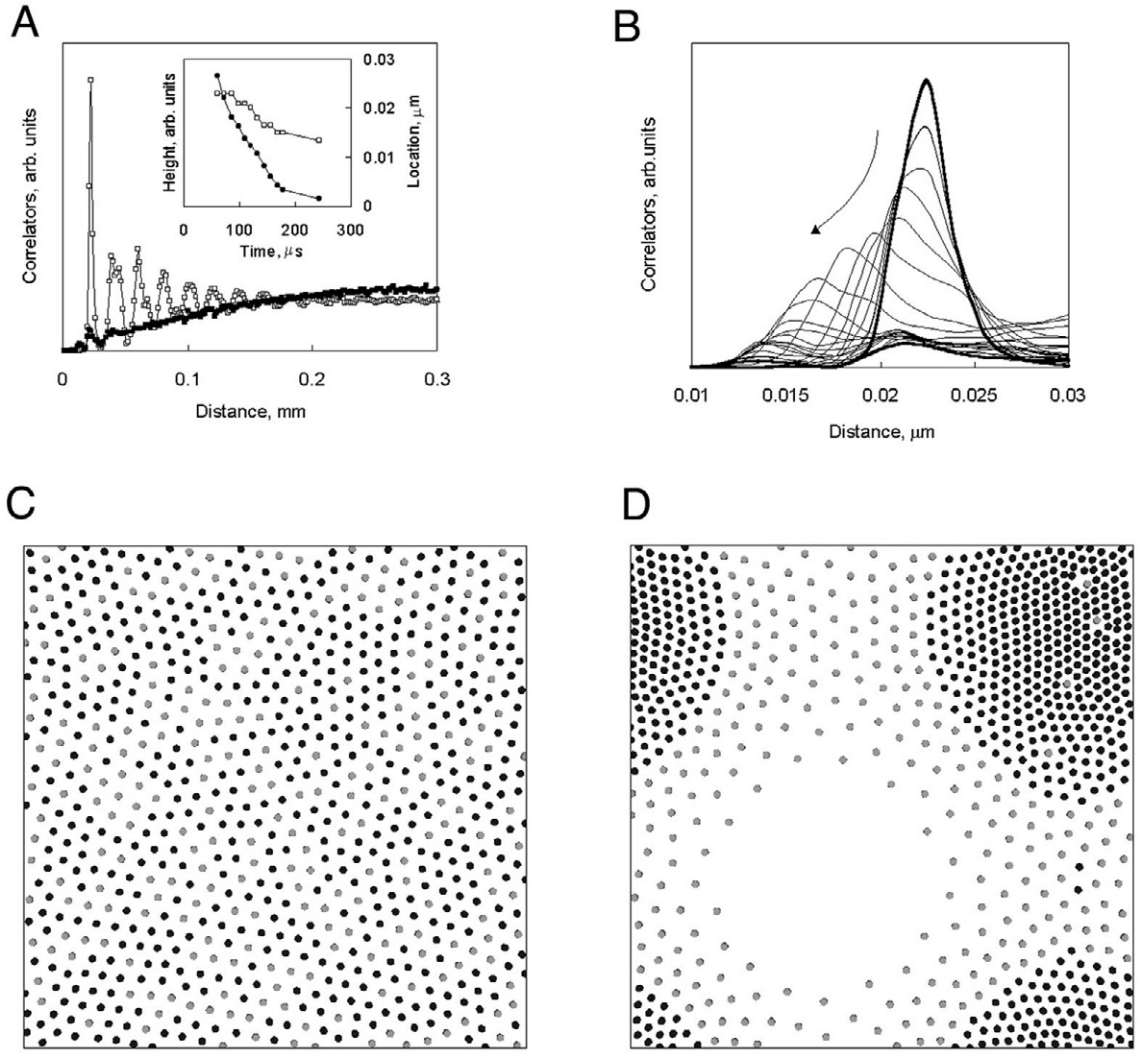

FIGURE 1 Simultaneous weak clustering and segregation. Attraction strength $\lambda = 1$, attraction radius $\zeta = 0.1$ μm, and Debye length $\xi = 0.06$ μm. (*A*) PSII-PSI correlation functions for the initial configuration (□) and the final configuration (■). (*Inset*) Time dependences of the height of the first maximum (●) of the correlation function and its location (□). (*B*) Shift of the first maximum of the correlation function in the course of time evolution from initial to final configuration. Arrow shows the direction of the shift of the first maximum. (*C*) Initial configuration. (*D*) Final configuration. For *C* and *D* black circles denote PSII positions and gray circles show PSI positions.

segregated quasi-crystalline structure. We note that in this phase the PSI-PSII, PSII-PSII, and PSI-PSI correlation functions (not shown) look the same, reflecting the absence of any segregation. When clustering occurs, the PSI-PSII correlation function (Fig. 3 *A*) retains some of the short-range order, acquiring at the same time a characteristic decrease starting at ~0.1 μm. The dynamics of the first maximum also shows an initial shift to lower values of the interparticle distance (initial to intermediate configurations, Fig. 3 *A*, *inset*, and Fig. 3 *B*). However, in this case this shift is accompanied by the growth of the first maximum amplitude.

Later, at ~50 μs, the segregation takes place, as the higher-charge PSI particles are pushed toward the periphery. The PSI-PSII correlation function (Fig. 3 *A*) acquires a clear maximum around 0.12 μm. The first maximum (Fig. 3 *A*, *inset*, and Fig. 3 *B*) shifts slightly back, with its amplitude noticeably decreasing. Finally the system arrives in a fully segregated state (Fig. 3 *D*), also manifested by the saturation of the dependences in Fig. 3 *A*, *inset*.

Clustering without segregation

This case is very hard to identify. The reason is that, if the attraction strength is decreased, the segregation processes are taking place much more slowly. Hence, when performing the computer experiments with finite systems, a situation with very long segregation times can be easily mistaken for clustering without segregation. In a way, the discussed

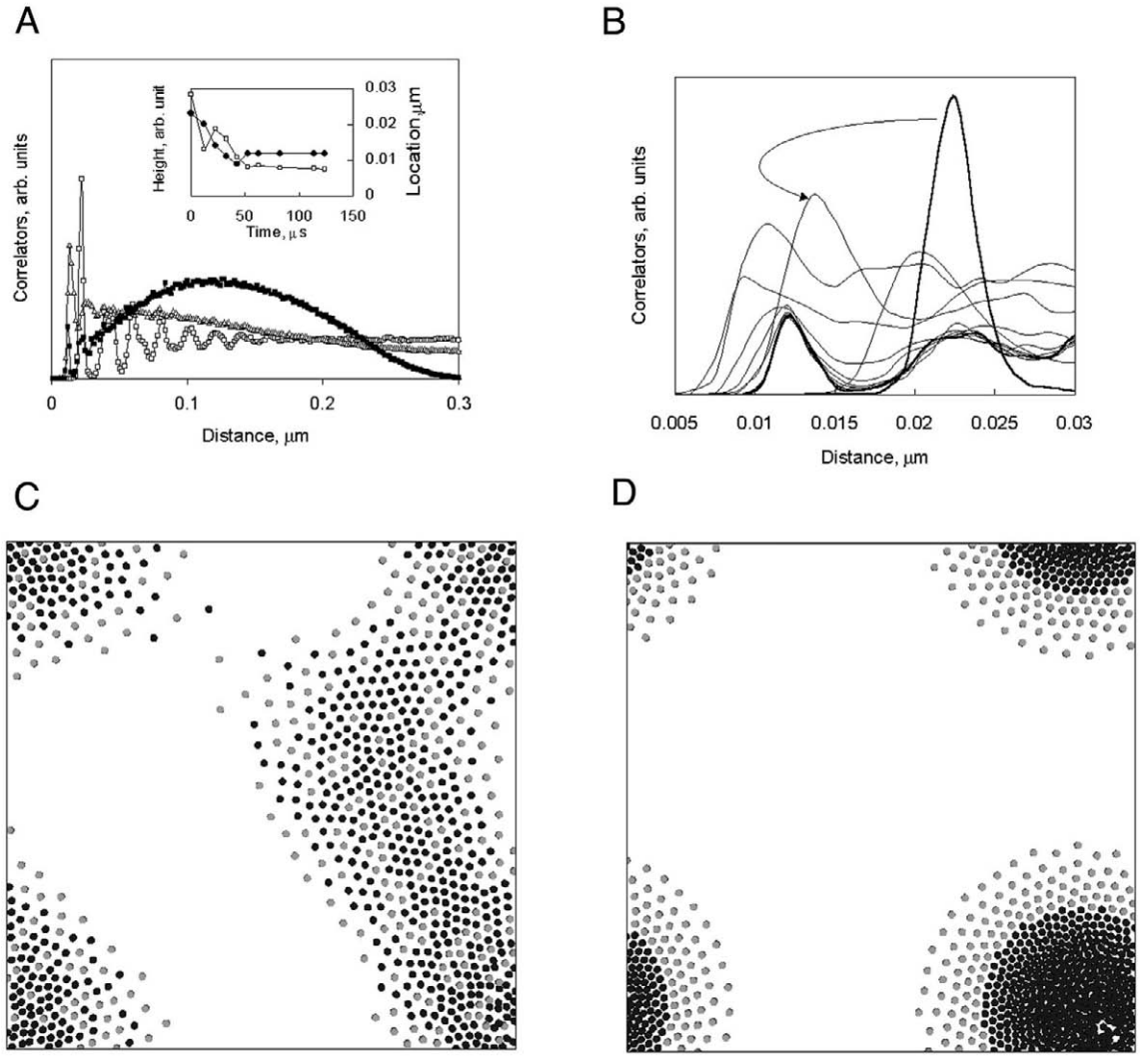

FIGURE 2 Simultaneous strong clustering and segregation. Attraction strength $\lambda = 1$, attraction radius $\zeta = 0.05$ μm, and Debye length $\xi = 0.02$ μm. (*A*) PSII-PSI correlation functions for the initial (□), the intermediate (△), and the final (■) configurations. (*Inset*) Time dependences of the height of the first maximum (●) of the correlation function and its location (□). (*B*) Shift of the first maximum of the correlation function in the course of time evolution from initial to final configuration through intermediate configuration (*broken line*). Arrow shows the direction of the shift of the first maximum. (*C*) Intermediate configuration. (*D*) Final configuration. For *c* and *d* black circles denote PSII positions and gray circles show PSI positions.

case is a certain limit of the above clustering with delayed segregation. Moreover, this case might also be difficult to identify experimentally, due to internal inhomogeneities pertinent to the in vivo systems.

Clustering without segregation, and later segregation at lower value of the Debye radius, are presented in Figs. 4-6. Results in Fig. 4 represent the effects of lowering the attraction strength to $\lambda = 0.2$ compared with $\lambda = 1$ for the case in Fig. 1, with the same attraction interaction radius ζ. Due to the weaker attraction, clustering can occur at lower value of the Debye radius $\xi = 0.01$ μm. The configurations presented in Fig. 4, *C* and *D*, show some signs of segregation, but no complete segregation occurs. Further calculations indicate that the situation shown in Fig. 4 *D* becomes frozen for rather long calculation times (not shown). The features of the PSI-PSII correlation function in Fig. 4, *A* and *B*, also support the direct visual perception of intermediate and final configurations. Specifically, the intermediate and the final state correlation functions (Fig. 4 *A*) are practically the same and show the same features as the intermediate case for clustering before segregation (Fig. 3 *A*). The same can be said about data in the inset in Fig. 4 *A*, although slight signs of back shifting of the first maximum location and slight decrease in its amplitude can be observed at a time of $\sim$100 μs.

Similar features may be observed in Fig. 5, although, due to the relatively weak attraction strength $\lambda = 0.1$ and short attraction range of $\zeta = 0.05$, the clustering takes place much

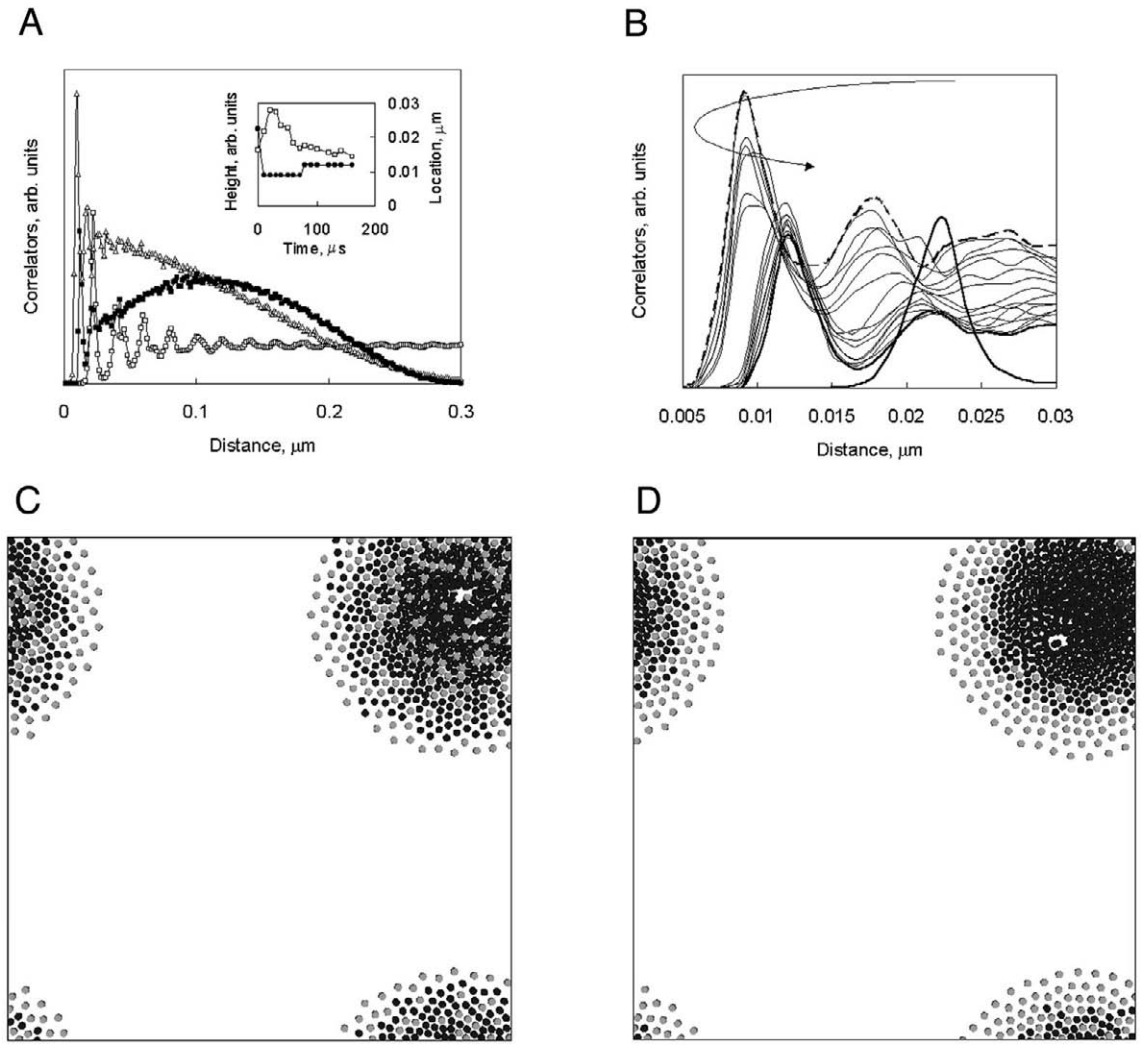

FIGURE 3 Strong clustering and later segregation. Attraction strength $\lambda = 0.3$, attraction radius $\zeta = 0.1$ μm, and Debye length $\xi = 0.01$ μm. Legend is as in Fig. 2.

more slowly, and at the times of observation no visible segregation can be identified. The intermediate situation (Fig. 5 *C*) is still within the time of clustering, which is clearly not yet complete in Fig. 4 *D*. Longer calculations did not show any cardinal changes in the situation and hence are not presented here. The PSI-PSII correlation functions' overall behavior is also characteristic of clustering without segregation, and so is the dynamics of the first maximum. This type of situation was previously observed by Rojdestvenski et al. (2000).

The situation provisionally labeled here as clustering without segregation is clearly a borderline case, as it avails segregation if the Debye radius ξ is further decreased (Fig. 6). A clear segregation pattern emerges as in the behavior of the PSI-PSII correlation function (Fig. 6 *A*), with a characteristic maximum at, in this case, 0.1 μm (see also Fig. 6, *C* and *D*). The first maximum shifts to greater distances and its height decreases accordingly (Fig. 6 *B*).

The above discussion is summarized in the two phase diagram sketches presented in Fig. 7. These are shown for two values of the attraction range ζ. Both plots (Fig. 7, *A* and *B*) are qualitatively similar, with a clearly identifiable non-segregated quasi-crystalline phase (white area above the curves) and clustered segregated states (light gray area below the curves). The borderline dark gray areas correspond to a possible stage of clustering without segregation, although for more clear understanding of what actually happens within this range of parameters, longer calculations for bigger systems are certainly needed.

CONCLUSIONS

In the present paper we model the kinetics and the equilibrium state of an ensemble of photosystems in thylakoid membranes as a classical many-body system with a com-

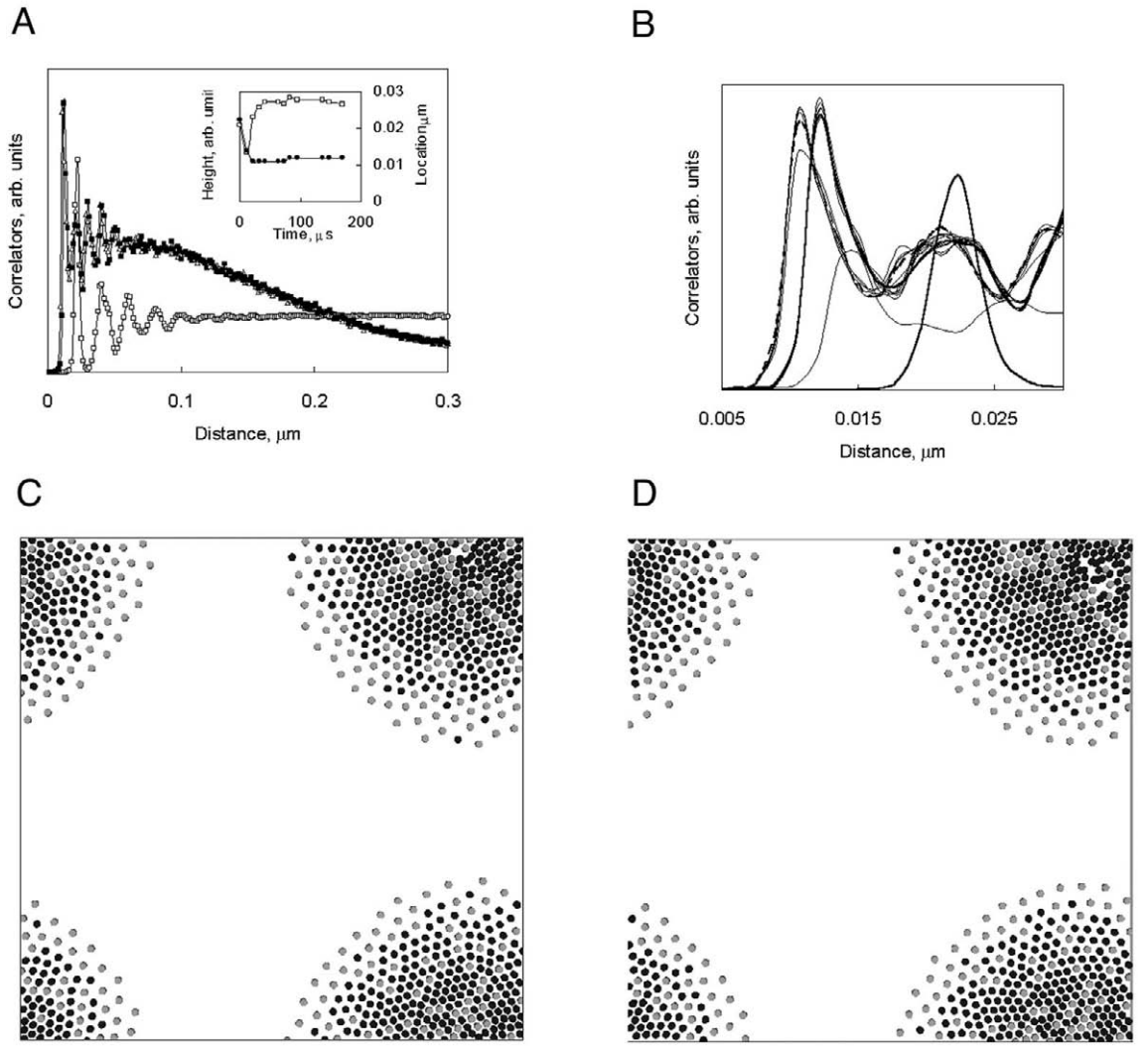

FIGURE 4 Strong clustering without segregation. Attraction strength $\lambda = 0.2$, attraction radius $\zeta = 0.1$ μm, and Debye length $\xi = 0.01$ μm. Legend is as in Fig. 2.

peting screened Coulomb repulsion and a lipid-induced attraction. We exploit the idea that segregation of photosystems within the membrane is a cooperative phenomenon similar to phase separation observed in the binary fluids (Poole et al., 1997). The ordering of photosystems within the membrane becomes the result of interplay between electrostatic interactions and lipid-mediated attraction. We should note that similar phenomena with, possibly, similar explanations are pertinent for other systems comprising lipid membranes and protein inclusions. One such example is lipid-mediated two-dimensional array formation of membrane bacteriorhodopsin (Sabra et al., 1998).

The main results of this paper can be formulated as follows. 1) We looked at the kinetics of the clustering and segregation in the PSI-PSII ensemble. Our previous results (Rojdestvenski et al., 2000) were mainly concerned with the equilibrium states of the ensemble with the given interactions. 2) We studied segregation and clustering in a wide range of parameters and found evidence for several possible scenarios of the phase transition. We also found evidence for possible time-scale hierarchy in segregation and clustering. Namely, at certain values of parameters the segregation occurs much more slowly than clustering. 3) We showed what changes to the PSI-PSII correlation functions correspond to different clustering and segregation scenarios. 4) We sketched phase diagrams of the system in the (λ, ξ) space and discussed the segregation slowdown in the regions close to the phase separation border (scenario 3).

We used a simple molecular dynamics method with variable time scales. A review of the application of molecular dynamics methods to study the kinetics of liquid phase and lipid membranes is given by Allen and Tildesley (1987) and Tieleman et al. (1997). However, the most detailed models applied in the study of lipid kinetics in the membranes avail

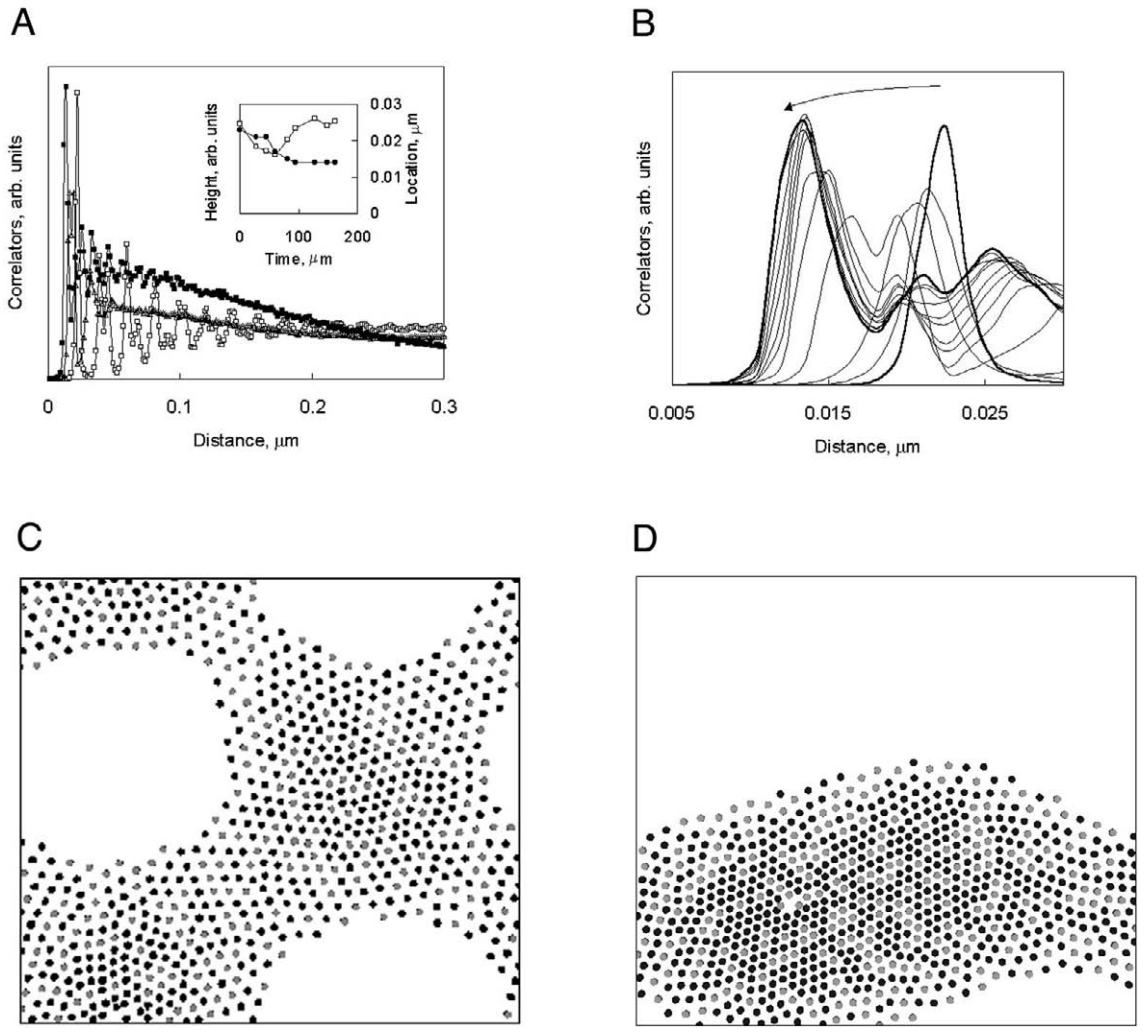

FIGURE 5 Weak clustering without segregation. Attraction strength $\lambda = 0.1$, attraction radius $\zeta = 0.05$ μm, and Debye length $\xi = 0.005$ μm. Legend is as in Fig. 2.

the time evolution of the system up to a few nanoseconds. The stacking and segregation phenomena manifest themselves at a time scale of seconds and at spatial scales of microns, which makes the utilization of simplified effective interactions unavoidable, especially if one is to study final distributions of photosystems at equilibrium. The use of a simplified model is backed by the fact that the segregation and stacking phenomena seem to be similar to a phase transition, so that the changes in structure are essentially macroscopic. In this case, the use of an approximate effective interaction is generally acceptable, if one is not preoccupied with calculating fine details of the phase transition, such as critical indices. As the correlation length increases in the vicinity of the transition point, the effective interaction is averaged over interacting domains of correlated molecules. In this case it is reasonable to assume that fine details of interaction, including any asymmetry of interaction, are averaged out, and a rather simple effective interaction may be put in place.

In this paper we describe the phase behavior of a system of pigment-protein complexes with only two types of interactions: segregative Coulomb-Debye repulsion and exponentially decaying lipid-induced attraction. In fact, there are many approaches in evaluating different types of protein-protein interactions within lipid bilayer membranes. Goulian et al. (1993) and Golestanian et al. (1996) describe several types of the pair-wise long-range lipid-membrane-induced interaction energy between foreign inclusions that are proportional to $1/r^4$, r being the distance between two inclusions. These interactions, depending on temperature, may be attractive or repulsive and, for large distances, is significant compared with electrostatic, VDW and other interactions. Some interactions are induced by the local or global elasticity of the membrane itself. For example, Dom-

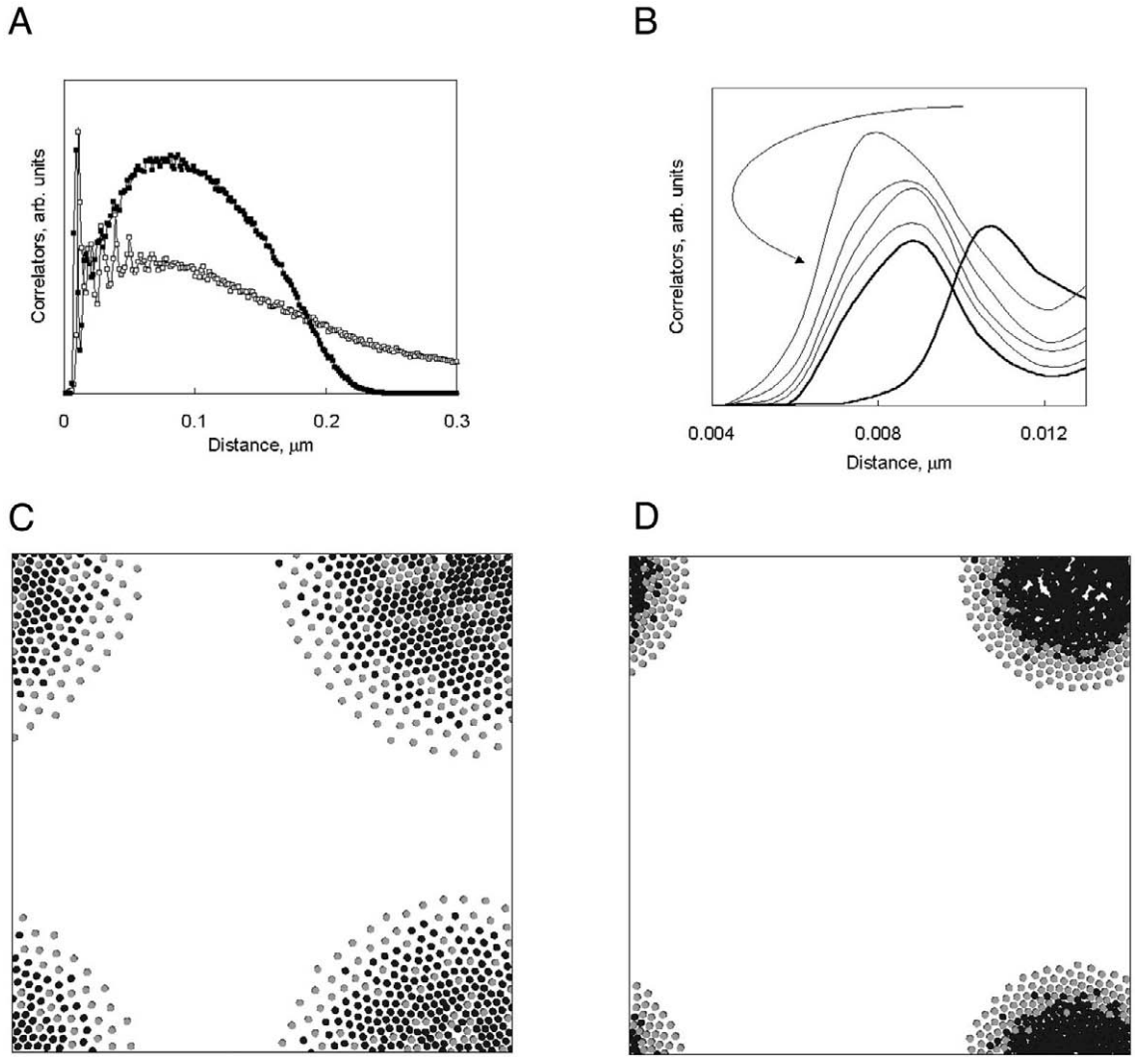

FIGURE 6 Segregation after strong clustering for lower ξ. Attraction strength $\lambda = 0.2$, attraction radius $\zeta = 0.1$ μm, and Debye length $\xi = 0.005$ μm. (*A*) PSII-PSI correlation functions for the initial configuration (□) and the final configuration (■). (*B*) Shift of the first maximum of the correlation function in the course of time evolution from initial through intermediate to final configuration. (*C*) Initial configuration. (*D*) Final configuration. For *C* and *D* black circles denote PSII positions and gray circles show PSI positions.

mersnes et al. (1998) present a theory of long-range elastic interactions between conical membrane inclusions in spherical vesicles. This interaction turns out to be repulsive and is proportional to the square of contact angle that is the angle between each inclusion and the membrane. One of the physical reasons for such kinds of interactions is a phenomenon of hydrophobic matching, extensively discussed in Gil et al. (1998) and Dumas et al. (1999). Some analytical computer simulations results also suggest that screening may overcompensate for the Coulomb repulsion so that the effective electrostatic interaction changes sign and becomes attractive, albeit short range (see, e.g., Arenzon et al., 2000; Hribar and Vlachy, 2000; and references therein).

It is a matter of further research to study how the explicit type of interaction affects the resulting clusterization, segregation, and the phase diagrams. We would expect, however, that in general, albeit with some exceptions, the clusterization and segregation phenomena are largely ruled by the fact that the system contains two types of competing interactions, attraction and repulsion, and that one or both types are selective, i.e., different for different types of photosystems. We demonstrate that electric charge mismatch of two photosystems can be a driving force in formation of protein complex arrays as well as a cause of their separation within the granum plane. Our simulations show that even the small difference in electric properties of photosystems provides appearance of quasi-crystalline arrays at small values of the Debye radius and contributes to photosystem segregation at intermediate ones. If photosystems have no electric charge or their charges are equal, lowering

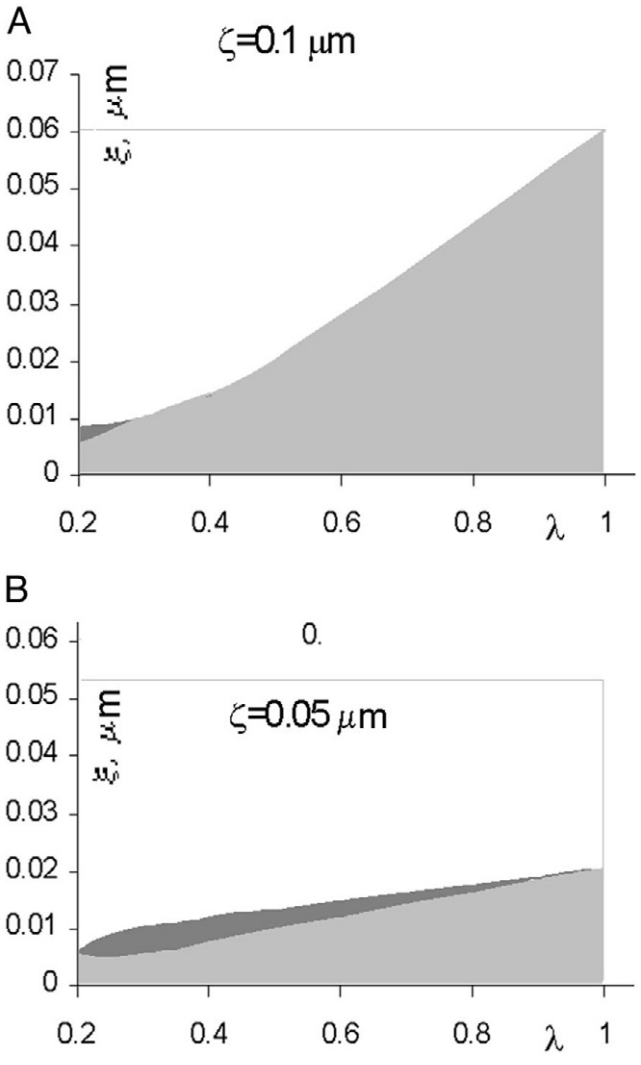

FIGURE 7 Phase behavior for $\zeta = 0.1$ μm (*A*) and $\zeta = 0.05$ μm (*B*). Light gray areas correspond to clustered and segregated configurations; white areas show disordered configurations. Dark gray areas show possible clustered states without segregation.

the Debye radius within the framework of our model results in protein cluster formation but particles show no segregation.

One more remark has to be made regarding our system being considered effectively infinite. It is known that lateral segregation is never observed in single membranes. This may be due to the fact that the segregation is, in general, slower than clustering. Clusterization creates inhomogeneities in the distributions of proteins, which may cause instability of the membrane, forming smaller vesicles. The experiments of this sort were discussed in Ivanov and Apostolova (1997) and Ivanov et al. (1987). The effect of divalent cations described in these papers involves simultaneous segregation (observed via changes in the spillover) and forming of smaller vesicles with concomitant stacking (observed visually). It would be interesting to check experimentally the hypothesis that the forming of smaller vesicles is preceded and caused by clustering as the result of stronger ionic screening.

This work was financially supported the Swedish Foundation for International Cooperation in Research and Higher Education (STINT), the Swedish Natural Science Research Council, Kempe Foundation, and the Natural Science and Engineering Research Council of Canada.

REFERENCES

Allen, J. F. 1992. How does protein phosphorylation regulate photosynthesis? *Trends Biol. Sci.* 17:12–17.

Allen, M. P., and D. J. Tildesley. 1987. Computer Simulation of Liquids. Oxford University Press, London.

Anderson, J. M. 1981. Consequences of spatial separation of photosystem 1 and 2 in thylakoid membranes of higher plant chloroplasts. *FEBS Lett.* 124:1–10.

Anderson, J. M. 1982. The significance of grana stacking in chlorophyll *b*-containing chloroplasts. *Photobiochem. Photobiophys.* 3:225–241.

Anderson, J. M. 1999. Insights into the consequences of grana stacking of thylakoid membranes in vascular plants: a personal perspective. *Aust. J. Plant Physiol.* 26:625–639.

Anderson, J. M., and B. Andersson. 1982. The architecture of photosynthetic membranes: lateral and transverse organization. *Trends Biol. Sci.* 7:288–292.

Anderson, J. M., and E. M. Aro. 1994. Grana stacking and protection of photosystem II in thylakoid membranes of higher plant leaves under sustained high irradiance: an hypothesis. *Photosynth. Res.* 41:315–326.

Andersson, B., and J. M. Anderson. 1980. Lateral heterogeneity in the distribution of chlorophyll-protein complexes of the thylakoid membranes of spinach chloroplasts. *Biochim. Biophys. Acta.* 593:427–440.

Arenzon, J. J., Y. Levin, and J. Stilk. 2000. The mean-field theory for attraction between like-charged macromolecules. *Physica A.* 283:1–5.

Barber, J. 1982. Influence of surface charges on thylakoid structure and function. *Annu. Rev. Plant Physiol.* 33:261–295.

Barber, J., and W. S. Chow. 1979. A mechanism for controlling the stacking and unstacking of chloroplast thylakoid membranes. *FEBS Lett.* 105:5–10.

Barber, J., W. S. Chow, C. Scoufflaire, and R. Lannoye. 1980. The relationship between thylakoid stacking and salt induced chlorophyll fluorescence changes. *Biochim. Biophys. Acta.* 591:92–103.

Ben-Tal, N., B. Honig, C. Miller, and S. McLauighin. 1997. Electrostatic binding of proteins to membranes. Theoretical predictions and experimental results with charybdotoxin and phospholipid vesicles. *Biophys. J.* 73:1717–1727.

Braintais, J. M., C. Vernotte, J. Olive, and F. A. Wollman. 1984. Kinetics of cation-induced changes of photosystem II fluorescence and of lateral distribution of the two photosystems in the thylakoid membranes of pea chloroplasts. *Biochim. Biophys. Acta.* 766:1–8.

Butler, W. L. 1978. Energy distribution in the photochemical apparatus of photosynthesis. *Annu. Rev. Plant Physiol.* 29:345–378.

Chow, W. S. 1999. Grana formation: entropy-assisted local order in chloroplasts? *Aust. J. Plant Physiol.* 26:641–647.

Chow, W. S., C. Miller, and J. M. Anderson. 1991. Surface charge, the heterogenous lateral distribution of the two photosystems, and thylakoid stacking. *Biochim. Biophys. Acta.* 1057:69–77.

Dobrikova, A. G., N. P. Tuparev, I. Krasteva, M. H. Busheva, and M. Y. Velitchkova. 1997. Artificial alterations of fluidity of pea thylakoid membranes and its effect on energy distribution between both photosystems. *Z. Naturforsch. C.* 52:475–480.

Dommersnes, P. G., J. B. Fournier, and P. Galatova. 1998. Long range elastic forces between membrane inclusions in spherical vesicles. *Europhys. Lett.* 42:233–238.

Drepper, F., I. Carlberg, B. Andersson, and W. Haehnel. 1993. Lateral diffusion of an integral membrane protein: Monte Carlo analysis of the migration of phosphorylated light-harvesting complex II in the thylakoid membrane. *Biochemistry.* 32:11915–11922.

Dumas, F., M. C. Lebrun, and J.-F. Tocanne. 1999. Is the protein/lipid hydrophobic matching principle relevant to membrane organization and function? *FEBS Lett.* 458:271–277.

Gennis, R. B. 1989. Biomembranes: Molecular Structure and Function. Springer-Verlag, New York.

Gil, T., J. H. Ipsen, O. G. Mouritsen, M. C. Sabra, M. M. Sperotto, and M. J. Zuckerman. 1998. Theoretical analysis of protein organization in lipid membranes. *Biochim. Biophys. Acta.* 1376:245–266.

Glazer, A. N., and A. Melis. 1987. Photochemical reaction centers: structure, organization, and function. *Annu. Rev. Plant Physiol.* 38:11–45.

Golestanian, R., M. Goulian, and M. Kadar. 1996. Fluctuation-induced interactions between rods on membranes and interfaces. *Europhys. Lett.* 33:241–245.

Goodchild, D. J., O. Bjorkman, and N. A. Pyliotis. 1972. Chloroplast ultrastructure, leaf anatomy and content of chlorophyll and soluble protein in rainforest species. *Carnegie Inst. Washington Year Book.* 71:102–107.

Goulian, M., R. Bruinsma, and P. Pincus. 1993. Long range forces in heterogeneous fluid membranes. *Europhys. Lett.* 22:145–150. Erratum: *Europhys. Lett.* 23:155.

Haehnel, W. 1984. Photosynthetic electron transport in higher plants. *Annu. Rev. Plant Physiol.* 35:659–693.

Haworth, P. 1983. Protein phosphorylation-induced state I-state II transition are dependent on thylakoid membrane microviscosity. *Arch. Biochem. Biophys.* 226:145–154.

Heimburg, T., and R. L. Biltonen. 1996. A Monte Carlo simulation study of protein-induced heat capacity changes and lipid-induced protein clustering. *Biophys. J.* 70:84–96.

Hribar, B., and V. Vlachy. 2000. Clustering of macroions in solutions of highly asymmetric electrolytes. *Biophys. J.* 78:694–698.

Israelachvili, J. N. 1992. Intermolecular and Surface Forces. Academic Press, London.

Ivanov, A. G. 1991. Phospholipase A2 induced effects on the structural organization and physical properties of pea chloroplast membranes. *Photosynth. Res.* 29:97–105.

Ivanov, A. G., and E. L. Apostolova. 1997. Multiple effects of sodium dodecylsulphate treatment on the chloroplast ultrastructure and membrane properties of pea thylakoids. *Plant Physiol. Biochem.* 35:235–243.

Ivanov, A. G., M. Velitchkova, and D. Kafalieva. 1987. Multiple effects of trypsin- and heat-treatment on the ultrastructure and surface charge density of pea chloroplast membranes. Influence on P700 parameters. *Prog. Photosynth. Res.* 2:741–744.

Izawa, S., and N. E. Good. 1966. Effects of salt and electron transport on the conformation of islated chloroplasts. II. Electron microscopy. *Plant Physiol.* 41:544–552.

Kleinschmidt, J. H., and D. Marsh. 1997. Spin-label electron spin resonance studies on the interactions of lysine peptides with phospholipid membranes. *Biophys. J.* 73:2546–2555.

Marcelja, S. 1976. Lipid-mediated protein interaction in membranes. *Biochim. Biophys. Acta.* 455:1–7.

Mouritsen, O. G., and M. Bloom. 1993. Models of lipid-protein interactions in membranes. *Annu. Rev. Biophys. Biomol. Struct.* 22:145–171.

Murata, N. 1969. Control of excitation transfer in photosynthesis. II. Magnesium independent distribution of excitation energy between two pigment systems in spinach chloroplasts. *Biochim. Biophys. Acta.* 189: 171–181.

Ojakian, G., and P. Satir. 1974. Particle movements in chloroplast membranes: quantitative measurements of membrane fluidity by freeze-fracture technique. *Proc. Natl. Acad. Sci. U.S.A.* 71:2052–2065.

Poole, P. H., T. Grande, C. A. Angell, and P. F. McMillan. 1997. Polymorphic phase transitions in liquids and glasses. *Science.* 275:322–323.

Quinn, P. J., and W. P. Williams. 1983. The structural role of lipids in photosynthetic membranes. *Biochim. Biophys. Acta.* 737:223–266.

Rojdestvenski, I., A. G. Ivanov, M. G. Cottam, and G. Öquist. 2000. A two-dimensional many body system with competing interactions as a model for segregation of photosystems in thylakoids of green plants. *Eur. Biophys. J.* 29:214–220.

Rubin, B. T., J. Barber, G. Paillotin, W. S. Chow, and Y. Yamamoto. 1981. A diffusional analysis of the temperature sensitivity of the Mg^{2+}-induced rise of chlorophyll fluorescence from pea thylakoid membranes. *Biochim. Biophys. Acta.* 638:69–74.

Sabra, M., J. Uitdehaag, and A. Watts. 1998. General model for lipid-mediated two-dimensional array formation of membrane proteins: application to bacteriorhodopsin. *Biophys. J.* 75:1180–1188.

Sintes, T., and A. Baumgartner. 1997. Protein attraction in membranes induced by lipid fluctuations. *Biophys. J.* 73:2251–2259.

Staehelin, L. A. 1986. Chloroplast structure and supramolecular organization of photosynthetic membranes. *Encycl. Plant Physiol.* 19:1–84.

Staehelin, L. A., and C. J. Arntzen. 1983. Regulation of chloroplast membrane function: protein phosphorylation changes the spatial organization of membrane components. *J. Cell Biol.* 26:781–786.

Stanley, H. E. 1988. Introduction to Phase Transitions and Critical Phenomena. Oxford University Press, New York.

Stys, D. 1995. Stacking and separation of photosystem I and photosystem II in plant thylakoid membranes: a physico-chemical view. *Physiol. Plant.* 95:651–657.

Tieleman, D. P., S. J. Marrink, and H. J. C. Berendsen. 1997. A computer perspective of membranes: molecular dynamics studies of lipid bilayer systems. *Biochim. Biophys. Acta.* 1331:235–270.

Trissl, H. W., and C. Wilhelm. 1993. Why do thylakoid membranes from higher plants form grana stacks? *Trends Biol. Sci.* 18:415–419.

White, S. H., and W. C. Wimley. 1999. Membrane protein folding and stability: physical principles. *Annu. Rev. Biophys. Biomol. Struct.* 28: 319–365.

Wollman, F. A., and B. Diner. 1980. Cation control of fluorescence emission, light scatter, and membrane stacking in pigment mutants of *Chlamidomonas reinhardtii. Arch. Biochem. Biophys.* 201: 646–658.

Wollman, F. A., L. Minai, and R. Nechushtai. 1999. The biogenesis and assembly of photosynthetic proteins in thylakoid membranes. *Biochim. Biophys. Acta.* 1411:21–85.

Yamamoto, Y. R., R. C. Ford, and J. Barber. 1981. Relationship between thylakoid membrane fluidity and the functioning of pea chloroplasts. *Plant Physiol.* 67:1067–1078.